AIAA JOURNAL
Vol. 45, No. 10, October 2007

Technical Notes

TECHNICAL NOTES are short manuscripts describing new developments or important results of a preliminary nature. These Notes should not exceed 2500 words (where a figure or table counts as 200 words). Following informal review by the Editors, they may be published within a few months of the date of receipt. Style requirements are the same as for regular contributions (see inside back cover).

Advances in the Characterization of Transient Two-Phase Flow

J. R. García-Cascales* and J. Mulas-Pérez*
Universidad Politécnica de Cartagena, 30202 Cartagena, Murcia, Spain
and
H. Paillère†
Commissariat à L'Énergie Atomique–Saclay, 91191 Gif-sur-Yvette Cedex, France

DOI: 10.2514/1.25644

Nomenclature

D	=	diameter, m
E	=	specific total energy, J/kg
e	=	specific internal energy, J/kg
F	=	flux vector
F^{nv}	=	nonviscous force, Pa/m
F_k^v	=	viscous friction, wall friction forces, Pa/m
f	=	friction factor
g	=	acceleration of gravity, 9.81 m/s
H	=	specific total enthalpy, J/kg
h	=	specific enthalpy, J/kg
k_u	=	numerical flux parameter
$\mathcal{L}$	=	latent heat ($h_g^{\mathrm{sat}} - h_f^{\mathrm{sat}}$), J/kg
L_h	=	tube length, m
M	=	Mach number
$\mathcal{P}$	=	advective upstream system models Mach number function
p	=	pressure, Pa
p_u	=	numerical flux parameter
q^i	=	heat exchanged with the interface, W/m^2
q^w	=	heat exchanged through the wall, W/m^2
u_k	=	velocity, m/s
x	=	vapor quality
z	=	axial coordinate
α	=	void fraction
Γ	=	net mass transfer flux through the interface, kg/m^3 s
ρ	=	density, kg/m^3
σ	=	numerical flux parameter
Ψ	=	vector introduced in the flux function definition

Subscripts

f	=	saturated liquid
g	=	saturated vapor
h	=	hydraulic
i	=	interface
k	=	any phase
L	=	left
l	=	liquid phase
m	=	mixture
R	=	right
r	=	relative
v	=	vapor phase
w	=	wall
$1/2$	=	interface between phases

Superscripts

c	=	convective
nv	=	nonviscous
p	=	pressure
sat	=	saturation
v	=	viscous

I. Introduction

THE study of two-phase flow mixtures is a difficult task to carry out, because there are many problems associated with the nonhyperbolic character of the system of equations: stiffness of source terms; discontinuities of the thermodynamic properties near the saturation lines (vapor or liquid); characterization of discontinuities such as shocks, rarefaction waves, or contact discontinuities; and so on. Problems also appear when one of the phases appears or disappears. In some of these cases, "tricks" are needed to go from a region in which there is only one phase to another in which there are two. In this Note, a combination of two two-phase models is developed to overcome this difficulty: namely, the one-pressure, six-equation model and the homogeneous equilibrium model. Furthermore, the AUSM$^+$-up scheme developed by Liou in [1] or [2] is extended to the analysis of transient two-phase flow. This study is restricted to mixtures of water and steam in which the disperse phase is supposed to be homogeneously distributed in the numerical cells studied.

II. System of Equations

The unsteady, one-dimensional, one-pressure, two-phase flow model is characterized by a set of balance equations for mass, momentum, and total energy. In the case of the separated model,

$$\frac{\partial}{\partial t}(\alpha\rho_v) + \frac{\partial}{\partial x}(\alpha\rho_v u_v) = \Gamma_v \tag{1a}$$

$$\frac{\partial}{\partial t}[(1-\alpha)\rho_l] + \frac{\partial}{\partial x}[(1-\alpha)\rho_l u_l] = \Gamma_l \tag{1b}$$

Received 29 August 2006; revision received 10 June 2007; accepted for publication 11 June 2007.

*Assistant Professor, Departamento Ingeniería Térmica y de Fluidos, Dr. Fleming, s/n.
†Researcher, Department of Modelling Structures and Systems (DM2S), Service of Fluids, Modelling and Studies (SFME), Laboratoire d'Etudes des Transferts et de Mécanique des Fluides.

$$\frac{\partial}{\partial t}(\alpha\rho_v u_v) + \frac{\partial}{\partial x}(\alpha\rho_v u_v^2 + \alpha p) = p^i\frac{\partial\alpha}{\partial x} + \alpha\rho_v g + F_v^{nv} + F_v^v + \Gamma_v u_i \tag{1c}$$

$$\frac{\partial}{\partial t}[(1-\alpha)\rho_l u_l] + \frac{\partial}{\partial x}[(1-\alpha)\rho_l u_l^2 + (1-\alpha)p] = -p^i\frac{\partial\alpha}{\partial x} + (1-\alpha)\rho_l g + F_l^{\mathrm{nv}} + F_l^v + \Gamma_l u_i \tag{1d}$$

$$\frac{\partial}{\partial t}(\alpha\rho_v E_v) + \frac{\partial}{\partial x}(\alpha\rho_v H_v u_v) = -p^i\frac{\partial\alpha}{\partial t} + \alpha\rho_v u_v g + q_v^i + q_v^w + \Gamma_v H_i \tag{1e}$$

$$\frac{\partial}{\partial t}[(1-\alpha)\rho_l E_l] + \frac{\partial}{\partial x}[(1-\alpha)\rho_l H_l u_l] = p^i\frac{\partial\alpha}{\partial t} + (1-\alpha)\rho_l u_l g + q_l^i + q_l^w + \Gamma_l H_i \tag{1f}$$

where p^i stands for the pressure difference between each phase and the interface [3], and

$$p^i = p - p_i = C^p\frac{\alpha(1-\alpha)\hat{\rho}_v\hat{\rho}_l}{\alpha\hat{\rho}_v + (1-\alpha)\hat{\rho}_l}(u_v - u_l)^2 \tag{2}$$

where p_i is the interfacial pressure,

$$\hat{\rho}_v = \rho_v + C^{vm}\rho, \qquad \hat{\rho}_l = \rho_l + C^{vm}\rho, \qquad \rho = \alpha\rho_v + (1-\alpha)\rho_l \tag{3}$$

C^p and C^{vm} are, respectively, an interfacial pressure correction and virtual mass parameters, and ρ is the mixture density. Densities are estimated by using tabulated equations of state of the form $\rho_v = \rho_v(p, h_v)$ or $\rho_l = \rho_l(p, h_l)$, where the vapor and liquid qualities are obtained by means of

$$x = x_v = \frac{1}{1 + [(1-\alpha)/\alpha](\rho_l/\rho_v)(u_l/u_v)}, \qquad x_l = 1 - x \tag{4}$$

and the speeds of sound are obtained by

$$c_k = \left(\frac{\partial\rho_k}{\partial h_k} + \frac{1}{\rho_k}\frac{\partial\rho_k}{\partial p_k}\right)$$

When a two-phase homogeneous equilibrium model is adopted, the set of equations of the mixture is given by [4]

$$\frac{\partial\rho}{\partial t} + \frac{\partial\rho u}{\partial x} = 0, \qquad \frac{\partial\rho u}{\partial t} + \frac{\partial(\rho u^2 + p)}{\partial x} = \rho g + \left(\frac{\partial p}{\partial z}\right)_F \qquad \frac{\partial\rho E}{\partial t} + \frac{\partial\rho H u}{\partial x} = \rho u g + q^w \tag{5}$$

where E, H, and u are mixture variables.

The velocity is given by

$$u = \frac{\alpha\rho_v u_v + (1-\alpha)\rho_l u_l}{\alpha\rho_v + (1-\alpha)\rho_l} \tag{6}$$

The heat exchanged through the wall is $q^w = q_l^w + q_v^w$. The speed of sound of the mixture is obtained by

$$c_m = \left(\alpha\frac{\rho}{\rho_v c_v^2} + (1-\alpha)\frac{\rho}{\rho_l c_l^2}\right)^{-1/2} \tag{7}$$

Other closure relationships need to be defined in systems (1) and (5). They will be described later, according to the test.

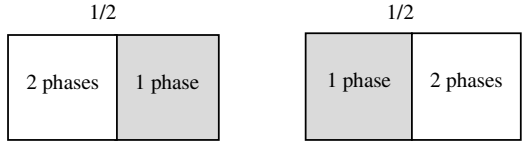

Fig. 1 Situation in which pressure flux is being underestimated.

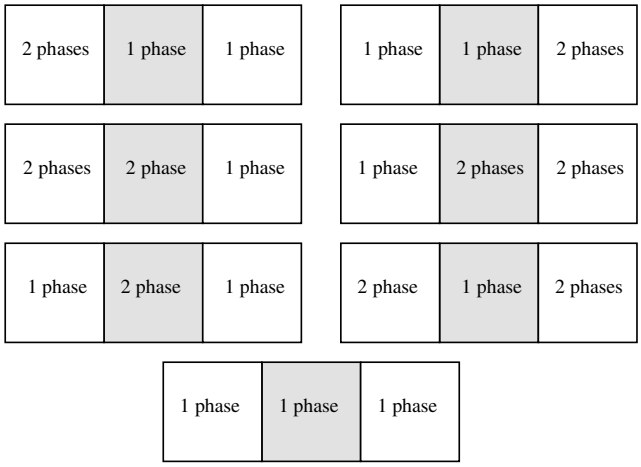

Fig. 2 Different possible combinations found in the 1-D analysis of unsteady two-phase flow.

III. Combination of the Homogeneous and Separated Models

Problems involving the appearance and disappearance of a phase are solved in many cases by code models that change from the separated model to the homogeneous model when a void-fraction threshold is reached [5]. In other cases, some dissipation is added to help the fluids disappear [6]. Previous works have shown some oscillations at the beginning or at the end of a phase change process. They are due to a wrong prediction of the pressure flux at the interface when some of the cases included in Fig. 1 take place in the analysis of a numerical benchmark. They are partially motivated by a misleading evaluation of the pressure term in the numerical flux. In this extension of the advective upstream system models (AUSM) numerical schemes to two-phase flow (AUSM$^+$-up), the problems appear as a consequence of the pressure flux definition. In the system of equations of phase k, the scheme may consider no pressure action on a cell without phase k, even though the nearest cell contains a certain amount of this phase.

Thus, the combination of the already presented two-phase models was thought to solve this problem. Because the homogeneous equilibrium model can only be used at low unsteady flows in which the velocity of vapor usually is not much higher than the velocity of the liquid [7], it will only be applied at the beginning or at the end of the processes of phase change when any of the cell combinations of Fig. 2 take place.

IV. Numerical Scheme

The AUSM$^+$-up scheme was extended to two-phase flow. It is characterized by its robustness when dealing with low Mach number flows, unlike previous explicit extensions of the AUSM$^+$ scheme to two-phase flow [4,8]. The basic idea of these schemes resides in the splitting of the flux vector into a convective part and a pressure part, such that for the phase k,

$$F_k = F_k^{(c)} + F_k^{(p)} \tag{8}$$

where $F_k^{(c)} = \dot{m}_k\Psi_k$, with $\dot{m}_k = \rho_k M_k c_k$, $M_k = u_k/c_k$,

$$\Psi = \begin{pmatrix} 1 \\ u_k \\ H_k \end{pmatrix}$$

and

$$F_k^p = \begin{pmatrix} 0 \\ \alpha_k p \\ 0 \end{pmatrix}$$

Dropping k for the sake of clarity, the numerical flux at the interface between two cells can be written as follows:

$$F_{1/2} = F_{1/2}^{(c)} + F_{1/2}^{(p)} \tag{9}$$

where $F_{1/2}^{(c)}$ if the numerical convective flux, and $F_{1/2}^{(p)}$ is the numerical pressure flux through the interface $1/2$. Therefore, for phase k, the numerical convective flux at each interface $1/2$ is given by

$$F_{1/2}^c = \dot{m}_{1/2}(u_L, u_R)\psi_{1/2}(u_L, u_R) \tag{10}$$

where

$$\psi_{1/2} = \begin{cases} \Psi_L, & \text{if } \dot{m}_{1/2} \geq 0 \\ \Psi_R, & \text{otherwise} \end{cases} \tag{11}$$

and pressure flux is given by $F_{1/2}^{(p)} = (0, p_{1/2}(u_L, u_R), 0)^t$.

These definitions are completed by defining the interface variables $\dot{m}_{1/2}$ and $p_{1/2}$ for each phase. They are based on polynomial functions of the left- and right-state Mach numbers. In the case of the AUSM$^+$-up scheme and for the phase k,

$$\dot{m}_{k1/2} = c_{k1/2} M_{k1/2} \begin{cases} \alpha_{kL}\rho_{kL}, & \text{if } M_{k1/2} > 0, \\ \alpha_{kR}\rho_{kR}, & \text{otherwise} \end{cases} \tag{12}$$

$$\begin{aligned} p_{1/2} = {} & \mathcal{P}_{(5)}^+(M_{kL})\alpha_{kL}p_{kL} + \mathcal{P}_{(5)}^-(M_{kR})\alpha_{kR}p_{kR} \\ & - k_u \mathcal{P}_{k(5)}^+(M_{kL})\mathcal{P}_{k(5)}^-(M_{kR})(\alpha_{kL}\rho_{kL} + \alpha_{kR}\rho_{kR}) \\ & \times (f_a c_{k1/2})(u_{kR} - u_{kL}) \end{aligned} \tag{13}$$

where $M_{k1/2}$, f_a, and the polynomials $\mathcal{P}_{(5)}^+$ and $\mathcal{P}_{(5)}^-$ can be found in Liou's works [1,2].

In the homogeneous model case, $\alpha_{kL,R}$ drops from all of the equations:

$$\dot{m}_{1/2} = c_{1/2} M_{1/2} \begin{cases} \rho_L, & \text{if } M_{1/2} > 0, \\ \rho_R, & \text{otherwise} \end{cases} \tag{14}$$

$$\begin{aligned} p_{1/2} = {} & \mathcal{P}_{(5)}^+(M_L)p_L + \mathcal{P}_{(5)}^-(M_R)p_R - k_u \mathcal{P}_{(5)}^+(M_L)\mathcal{P}_{(5)}^-(M_R) \\ & \times (\rho_L + \rho_R)(f_a c_{1/2})(u_R - u_L) \end{aligned} \tag{15}$$

V. Numerical Results

Two numerical benchmarks introduced in [9] were considered: a fast-depressurization test and a boiling-flow problem. In all of these tests, the values of the interfacial-pressure-correction parameters are $C^p = 2$ and $C^{\text{vm}} = 0$, and 1-D meshes of 100 cells are used in the calculations.

A. Fast Depressurization: Super Canon

This test consists of a fast-depressurization process that takes place in a horizontal tube filled with liquid water at high pressure. At time $t = 0$, one end of the tube is opened and a pressure drop from 150 to 1 bar takes place in about 0.5 s. During this process, the liquid flashes and a pressure wave propagates from the break opening to the far end of the tube in the two-phase mixture.

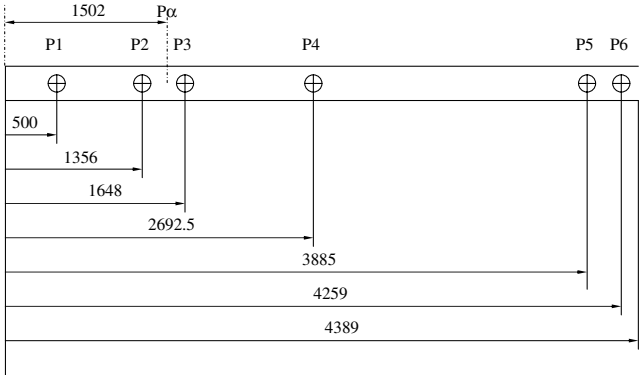

Fig. 3 Test geometry.

The tube is 4.389 m in length and 100 mm in diameter (Fig. 3). The initial conditions are characterized by a pressure of $p = 150$ bar, a void fraction of $\alpha = 0$, a liquid velocity of $u_l = 0$, and a liquid temperature of $T_l = 300°\text{C}$. At the open end, boundary conditions are defined by a discharge pressure at 1 bar.

The physical processes were characterized as follows:

Interfacial heat transfer:

$$\begin{aligned} & q_l = \frac{C_\tau}{\tau}\alpha(1-\alpha)\rho_l(h_l^{\text{sat}} - h_l), \\ & q_v = \frac{C_\tau}{\tau}\alpha(1-\alpha)\rho_v(h_v^{\text{sat}} - h_v), \qquad \Gamma_v = -\frac{q_v + q_l}{h_v^{\text{sat}} - h_l^{\text{sat}}}, \\ & \Gamma_l = -\Gamma_v \end{aligned} \tag{16}$$

where $C_\tau = 1$, $\tau = 3 \times 10^{-3}$ s u$^i = \alpha \text{u}_v + (1-\alpha)u_l$, $h_{vi} = h_v^{\text{sat}}$, and $h_{li} = h_l^{\text{sat}}$ (expressions proposed in [10]).

Nonviscous friction:

$$\boldsymbol{F}_v^{\text{nv}} = \tfrac{1}{8} C_D a^{\text{int}} |\boldsymbol{u}_r| \cdot \boldsymbol{u}_r, \qquad \boldsymbol{F}_l^{\text{nv}} = -\boldsymbol{F}_v^{\text{nv}} \tag{17}$$

where $C_D = 0.44$, $r_{\text{sm}} = 0.5$, and $a^{\text{int}} = [3\alpha(1-\alpha)]/r_{\text{sm}}$.

Viscous friction:

$$\boldsymbol{F}_v^v = -\frac{f}{D_h}\frac{\alpha\rho_v|\boldsymbol{u}_v| \cdot \boldsymbol{u}_v}{2}, \qquad \boldsymbol{F}_l^v = -\frac{f}{D_h}\frac{(1-\alpha)\rho_l|\boldsymbol{u}_l| \cdot \boldsymbol{u}_l}{2} \tag{18}$$

where $f = 0.017$.

The vapor-velocity and void-fraction distributions along the tube were calculated at the beginning of the flashing process with the AUSM$^+$-up and AUSM$^+$ schemes. Figures 4 and 5 compare the values of these variables at times $t = 0.005$ and 0.01 s. The oscillations that appeared with the AUSM$^+$ scheme disappear with the AUSM$^+$-up scheme, which includes the algorithm already presented (if any of the situations in Fig. 2 take place, the homogeneous model is used; otherwise, the six-equation model is used).

B. Boiling Flow in a Uniformly Heated Vertical Channel

This test consists of a vertical channel with an upward flowing water stream that is heated uniformly by means of an external heat source. The geometry used is a channel with a length $L_h = 3.65$ m and a diameter $D_h = 0.0142$ m. Initial conditions were imposed by saturated liquid state at the inlet so that boiling starts at the inlet. In addition, $\alpha = 0$, $p = 69$ bar, and $h_l = h_f$ (69 bar).

Boundary conditions at the inlet are characterized by the previous liquid enthalpy; $u_l = 0.7802$ m/s and $\alpha = 0$. The outlet is defined by a discharge pressure of 69 bar.

The closure laws are the following:

1) Drag force is given by Eqs. (17).

2) Wall friction was modeled as

$$\boldsymbol{F}_v^v = -\frac{f}{D_h}\frac{\alpha\rho_l|\boldsymbol{u}_l| \cdot \boldsymbol{u}_l}{2}, \qquad \boldsymbol{F}_l^v = -\frac{f}{D_h}\frac{(1-\alpha)\rho_l|\boldsymbol{u}_l| \cdot \boldsymbol{u}_l}{2} \tag{19}$$

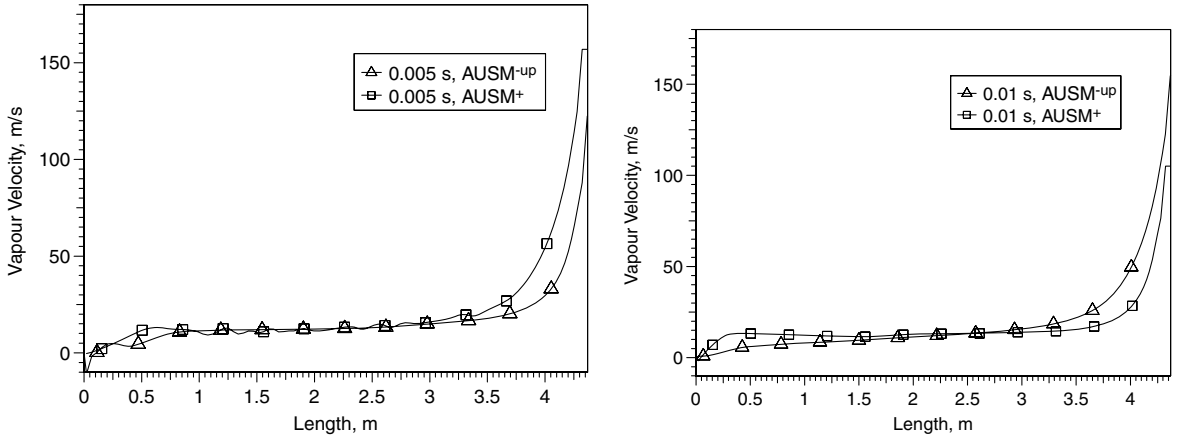

Fig. 4 Fast-depressurization test; AUSM$^+$-up vs AUSM$^+$ during the onset of the flashing process.

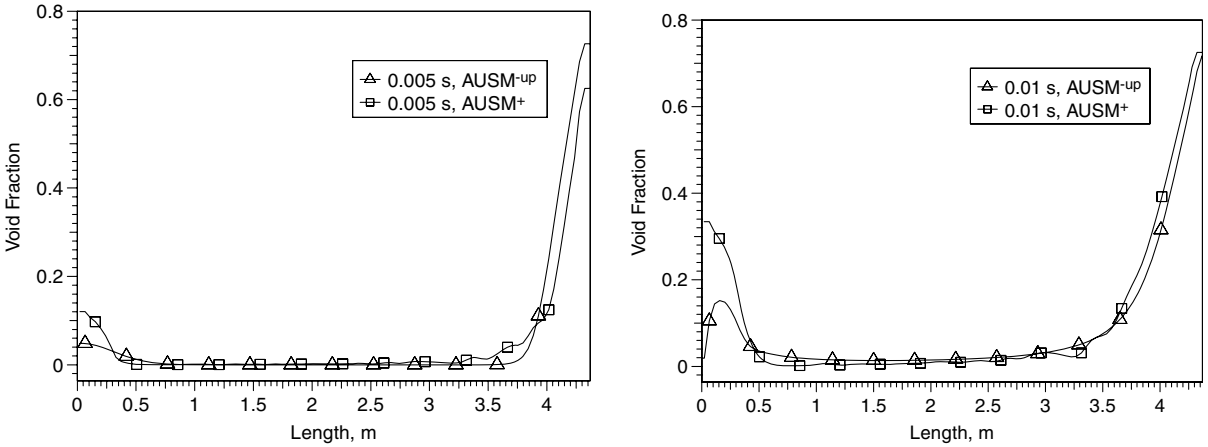

Fig. 5 Fast-depressurization test; AUSM$^+$-up vs AUSM$^+$ during the onset of the flashing process.

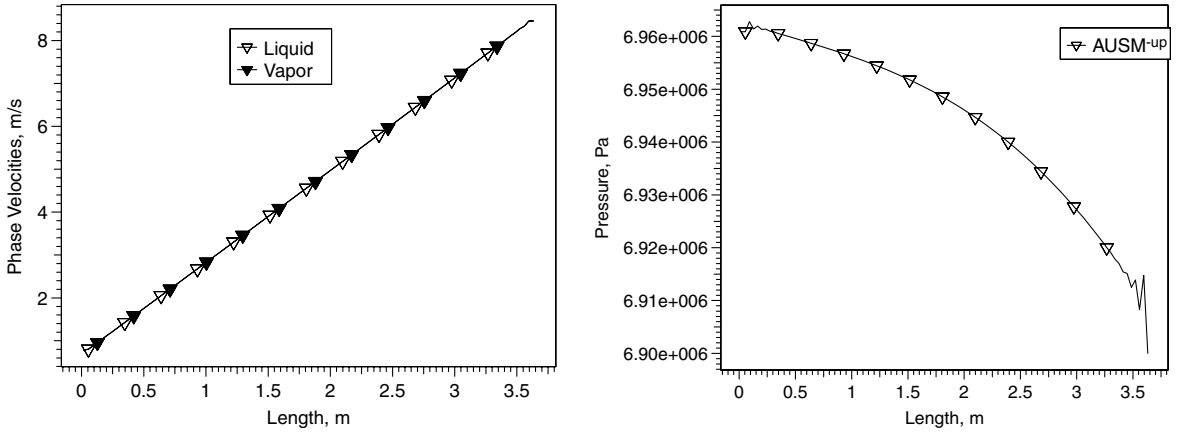

Fig. 6 Boiling-channel test; steady-state solution for several variables, vapor and liquid velocities (left) and pressure (right).

3) Wall heat transfer was added by means of

$$q_i = N_{\mathrm{PCH}} \frac{\mathcal{L}}{L_h v_{\mathrm{fg}}} \tag{20}$$

where $N_{\mathrm{PCH}} = 10$ and initial velocity $u_0 = 0.7802$ m/s.

4) Interfacial mass transfer is

$$\Gamma = \begin{cases} 0 & \text{if } T_l < T_f, \\ \frac{q^i}{L} & \text{otherwise} \end{cases} \tag{21}$$

The profiles of vapor and liquid velocities and pressure are depicted at steady state in Fig. 6. These results have been calculated

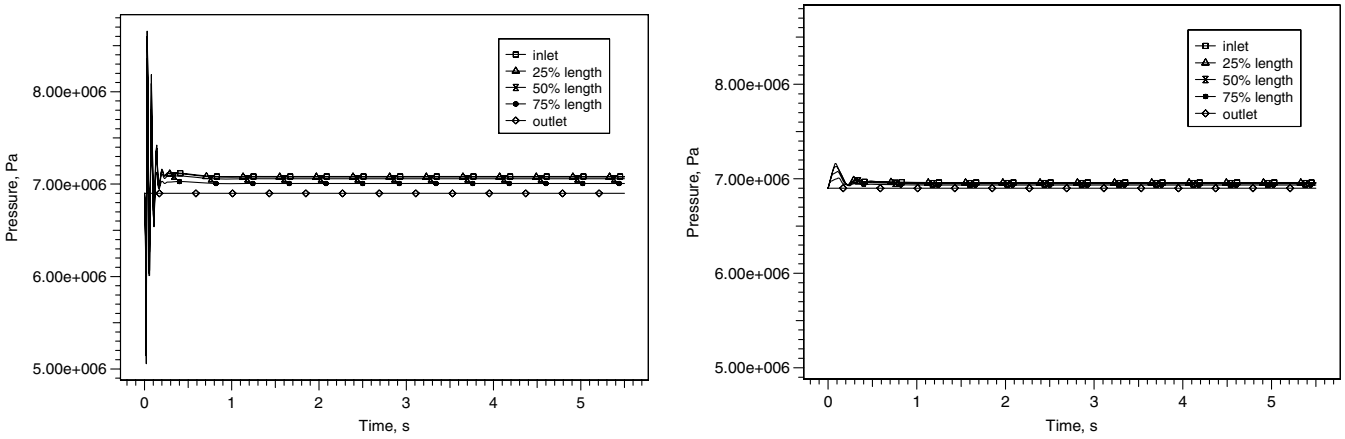

Fig. 7 Boiling-channel test; pressure computed at different points of the duct with two different schemes, AUSM$^+$ (right) and AUSM$^+$-up with the algorithm already presented (left).

by using the AUSM$^+$-up scheme. Both velocities are equally a clear example of homogeneous flux, because the slip ratio $u_v/u_l = 1$.

At the inlet, oscillations in pressure and velocity reported in [8] were eliminated with the new algorithm: it was mostly at first instants that vapor began to appear. At the outlet, some oscillations still remained in the pressure profile. Figure 7 shows the results obtained for the pressure at different positions, with AUSM$^+$ and AUSM$^+$-up including the new algorithm. In the second case, the initial oscillations were practically suppressed.

VI. Conclusions

In this work, a new algorithm to characterize transient two-phase flow with phase change was implemented successfully. Despite the fact that the method is not very orthodox, it avoids certain spurious oscillations in the computation of the characteristic variables of the flow when a phase appears or disappears. The results obtained with this algorithm improve upon those obtained with other upwind numerical schemes extended to two-phase flow by the authors.

Furthermore, the ability of the AUSM$^+$-up scheme to compute fast-depressurization processes accompanied by a flashing of the liquid phase was proven. Although the interfacial mass transfer term is quite simple, this phenomenon and the pressure-wave propagation into the two-phase mixture were modeled properly. The strong coupling between pressure and void fraction has also been suitably characterized. The numerical solutions do not match well with the experimental data, but this is attributed to the unadjusted physical models used in these simulations. In the solution of problems with stiff source terms, viscous friction, nonviscous friction and heat transfer terms, such as those already considered, the performance of the scheme is fairly satisfactory. The scheme is also able to predict the pressure drop at steady state, the volume fraction at the exit, and the onset of boiling. As in other contributions, some spurious oscillations appear in the pressure field at the outlet and at the point at which the onset of boiling takes place. They can be reduced by refining the mesh at such critical points. The scheme works quite well at any speed.

References

[1] Liou, M. S., "A Further Development of the AUSM$^+$ Scheme Toward Robust and Accurate Solutions for All Speeds," 16th AIAA Computational Fluid Dynamics Conference, Orlando, FL, AIAA Paper 2003-4116, June 2003.

[2] Liou, M. S., "A Sequel to AUSM, Part 2: AUSM$^+$-up for All Speeds," *Journal of Computational Physics*, Vol. 214, No. 1, May 2006, pp. 137–170.

[3] Bestion, D., "The Physical Closure Laws in the CATHARE Code," *Nuclear Engineering and Design*, Vol. 124, No. 3, Dec. 1990, pp. 229–245.

[4] Paillère, H., Kumbaro, A., Viozat, C., Clerc, S., Broquet, A., and Corre, C., "A Comparison of Roe, VFFC and AUSM$^+$ Schemes for Two Phase Water/Steam Flows," *Godunov Methods: Theory and Applications*, edited by E. F. Toro, Kluwer Academic, Norwell, MA, and Plenum, New York, 2000.

[5] Bestion, D., "The Phase Appearance and Disappearance in the CATHARE Code," *Proceedings of the Conference Trends in Numerical and Physical Modeling for Industrial Multiphase Flows* [CD-ROM], Ecole Normale Supérieure de Cachan, Cachan, France, 2000; also available online at http://www.cmla.ens-cachan.fr/Cmla/Perfortmans/.

[6] Paillère, H., Corre, C., and García-Cascales, J. R., "On the Extension of the AUSM$^+$ Scheme to Compressible Two-Fluid Models," *Computers and Fluids*, Vol. 32, No. 6, July 2003, pp. 891–916

[7] Whalley, P. B., *Two Phase Flow and Heat Transfer*, Oxford Univ. Press, New York, 1996.

[8] García-Cascales, J. R., and Paillère, H., "Application of AUSM Schemes to Multi-Dimensional Compressible Two-Phase Flow Problems," *Nuclear Engineering and Design*, Vol. 236, No. 12, June 2006, pp. 1225–1239.

[9] Mimouni, S., De Cachard, F., García-Cascales, J. R., Deconinck, H., Franchello, G., Graf, U., Kumbaro, A., Paillere, H., Ricchiuto, M., Romenski, E., Romstedt, P., Smith, B., Städtke, H., Toro, E.F., and Worth, B., "Advanced Three-Dimensional Two-Phase Flow Simulation Tool for Application to Reactor Safety (ASTAR): Benchmarking of Test Cases," *Proceedings of the ASTAR International Workshop on Advanced Numerical Methods for Multidimensional Simulation of Two-Phase Flow* [CD-ROM], Gesellchaft für Anlagen- und Reaktorsicherheit (GRS), Garching, Germany, 2003.

[10] Toumi, I., "An Upwind Numerical Method for Two Fluid Two Phase Flow Models," *Nuclear Science and Engineering*, Vol. 123, No. 2, June 1996, pp. 147–168.

S. Aggarwal
Associate Editor